

T. Cariou<sup>1</sup>, Y. Bozec<sup>2</sup>, J.P. Gac<sup>2</sup>, C. Guillerm<sup>3</sup>, E. Macé<sup>2</sup>, P. Marrec<sup>4</sup>, M. Vernet<sup>2</sup>.  
<sup>1</sup> Sorbonne Universités, UPMC Univ Paris 06, CNRS, Fédération de Recherche (FR2424), Station Biologique de Roscoff, 29680, Roscoff, France.  
<sup>2</sup> Sorbonne Universités, UPMC Univ Paris 06, CNRS, UMR 7144, Station Biologique de Roscoff, 29680, Roscoff, France.  
<sup>3</sup> Division technique de l'INSU, Plouzané,  
<sup>4</sup> Aix Marseille Univ, Université de Toulon, CNRS, IRD, MIO UM 110, Marseille, France, 13288, Marseille, France,

The actual development of monitoring networks, in coastal areas, provides to the scientific community platforms to deploy and test new sensors. In 2007, the Marine Chemistry team, in Roscoff equipped the cardinal buoy of opportunity ASTAN (picture 1) (Western Channel) from the French "Maritime aids to navigation and lighthouse Authorities" with a full CTD system (temperature, salinity, D.O., fluorescence) and atmospheric sensors. Cycles measurements occur every 30 minutes. To complete the existing system, we installed in 2015 a pCO<sub>2</sub> sensor from Sunburst Sensors LLC (picture 2). This sensor uses indicator-based spectrophotometric method to measure the environment pCO<sub>2</sub> variations by diffusion through a membrane.

### Principle :

The SAMI pCO<sub>2</sub> analysis is based on the colorimetric changes of a pH sensitive indicator solution (Bromothymol Blue). Aqueous carbon dioxide in seawater diffuses across the silicon membrane equilibrator (Fig. 2) and modifies the equilibrated indicator solution :  $\text{HI}^- \rightleftharpoons \text{H}^+ + \text{I}^{2-} (\text{Ka}') \text{ where } \text{HI}^- \text{ and } \text{I}^{2-} \text{ are the protonated and unprotonated forms of the diprotic indicator, Ka' the apparent indicator equilibrium constant. The absorbance measurements are made at the absorbance maxima of HI}^- (434 \text{ nm}) \text{ and } \text{I}^{2-} (620 \text{ nm}) (Fig. 1).$

$$\text{pH} = \text{pKa}' + \log\left(\frac{[\text{I}^{2-}]}{[\text{HI}^-]}\right) \text{ with } \frac{[\text{I}^{2-}]}{[\text{HI}^-]} = \frac{A_R \frac{\epsilon_{620a}}{\epsilon_{434a}}}{\frac{\epsilon_{620b}}{\epsilon_{434b}} - A_R \frac{\epsilon_{434b}}{\epsilon_{434a}}}, A_R = A_{620}/A_{434} \text{ and } \epsilon' \text{'s are ratios of the HI}^- \text{ and } \text{I}^{2-} \text{ molar absorptivities.}$$

The instrument response  $\text{RCO}_2 = -\log\left(\frac{A_R \frac{\epsilon_{620a}}{\epsilon_{434a}}}{\frac{\epsilon_{620b}}{\epsilon_{434b}} - A_R \frac{\epsilon_{434b}}{\epsilon_{434a}}}\right) = \text{pKa}' - \text{pH}$ . The response RCO<sub>2</sub> is

therefore only dependent upon the molar absorptivities ( $\epsilon'$ 's) and absorbance ratio A<sub>R</sub>. To calculate A<sub>R</sub>, the optical absorbances at 434 and 620 nm are corrected by regular measurements of a blank solution (de-ionized water) at 740 nm.

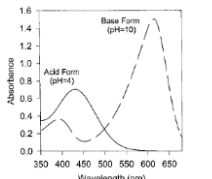


Fig. 1: Optical spectrum of bromothymol blue

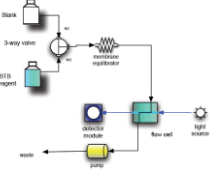


Fig. 2: SAMI system diagram



Picture 1 : Astan Buoy, off Roscoff - (© W. Thomas)



Picture 2 : SAMI installation under Astan Buoy - (© W. Thomas)

### Calibration :

The SAMI response (RCO<sub>2</sub>) is determined using a calibrated Li-COR (NDIR) CO<sub>2</sub> analyzer. Variable CO<sub>2</sub> gas concentrations are monitored in a thermostated chamber. The SAMI and NDIR data are combined to give a second-order polynomial calibration curve.  $\text{RCO}_2 = a(\log\text{pCO}_2)^2 + b(\log\text{pCO}_2) + c$  (Fig.3). A temperature coefficient is also determined to correct the pCO<sub>2</sub> value at temperature differing from the calibration temperature. Then, sensor values are compared to measurements in a bath using again the Li-COR (NDIR) CO<sub>2</sub> analyzer (Fig.4).

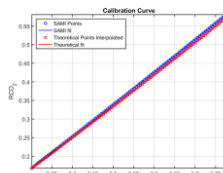


Fig. 3: SAMI calibration curves

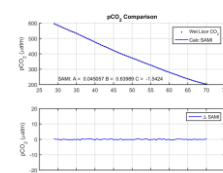


Fig. 4 : Comparison with Li-COR CO<sub>2</sub> analyzer

## 2016 - RESULTS

### Seasonal variability of pCO<sub>2</sub> and dissolved oxygen (D.O.) Astan Buoy - 2016

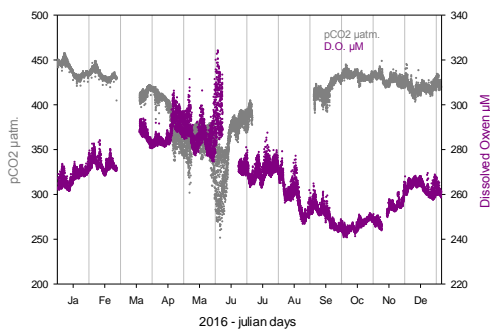


Fig. 5 : 2016 pCO<sub>2</sub> and D.O. variability

### Seasonal variability of seawater temperature, salinity and fluorescence. Astan Buoy - 2016

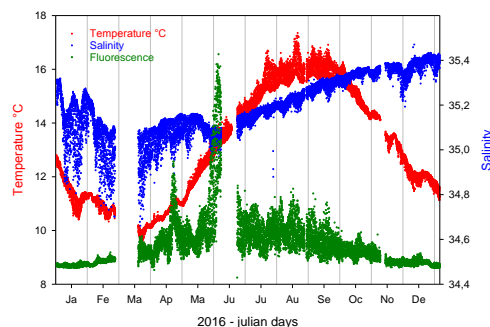


Fig. 6 : 2016 seawater temperature, salinity and fluorescence variability

### Variability of seawater temperature, salinity and fluorescence. Astan buoy - Winter 2016

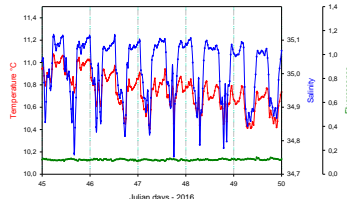


Fig. 10: Winter seawater temperature, salinity and fluorescence variability

### Variability of pCO<sub>2</sub> and dissolved oxygen (D.O.) Astan buoy - Winter 2016

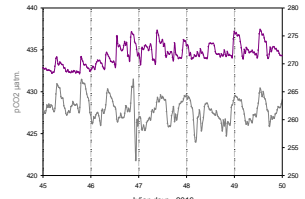


Fig. 7: Winter pCO<sub>2</sub> and D.O. variability

### Variability of seawater temperature, salinity and fluorescence. Astan Buoy - Spring 2016

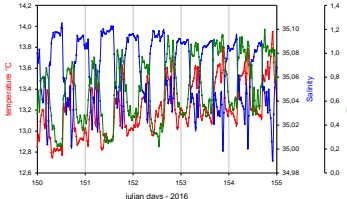


Fig. 11: Spring seawater temperature, salinity and fluorescence variability

### Variability of seawater pCO<sub>2</sub> and dissolved oxygen (D.O.) Astan buoy - Spring 2016

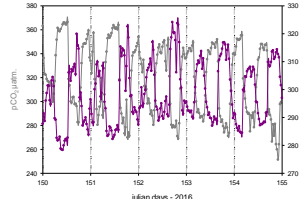


Fig. 8: Spring pCO<sub>2</sub> and D.O. variability

### Variability of seawater temperature, salinity and fluorescence. Astan Buoy - Fall 2016

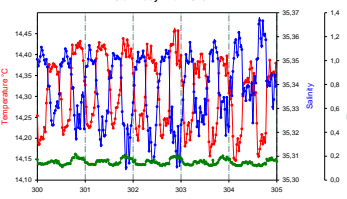


Fig. 12: Fall seawater temperature, salinity and fluorescence variability

### Variability of seawater pCO<sub>2</sub> and dissolved oxygen (D.O.) Astan Buoy - Fall 2016

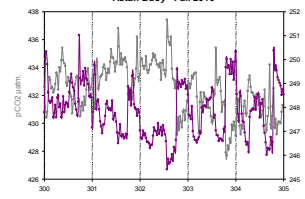


Fig. 9: Fall pCO<sub>2</sub> and D.O. variability

**Conclusion :** Results obtained with SAMI and the other sensors highlight the dynamics of this ecosystem (Fig.5 to 12). The seasonal variability of the biogeochemical parameters of the coastal area is well captured by the system. SAMI allows to measure the amounts of pCO<sub>2</sub> of the natural environment which behaves like source or sink of carbon depending on the seasons (solubility or/and biological pumps). We can also notice the strong daily variability of the parameters influenced by the tidal currents .